Efficient Size and Heading Angle Estimation of Ships in SAR and ISAR Images

Sushil Kumar Joshi, *Member, IEEE*, Stefan V. Baumgartner, *Senior Member, IEEE* and Björn Tings

***Abstract*—For maritime security applications it is advantageous or even required, that additionally to the geographical positions and moving directions the dimensions of the detected ships are available for subsequent classification and recognition purposes. In this paper a fast and robust method for size and heading angle estimation of ships in synthetic aperture radar (SAR) and inverse SAR (ISAR) images is proposed. The novel method leverages the eigenvalue decomposition of the detected ship pixel positions for determining the just mentioned parameters. The effectiveness of the proposed method is assessed against several state-of-the-art methods by using real X-band SAR images acquired with the German TerraSAR-X radar satellite in stripmap mode. The achieved accuracies of the proposed method are better than the ones obtained with the considered state-of-the-art methods and, as a further benefit, the computation time is also significantly shorter.**

***Index Terms*—ships, spaceborne, synthetic aperture radar (SAR), maritime security.**

I. INTRODUCTION

SHIP detection and monitoring of ship traffic are imperative for ensuring maritime safety and security, combating various maritime threats including piracy, illegal fishing and unauthorized immigration. Air- and spaceborne radar sensors with their weather-independent and day-night data acquisition capabilities are well-suited for these tasks [1]. Furthermore, beyond mere detection, the proliferation of these sensors with enhanced resolution and the advancement in image processing technology facilitates the estimation of additional ship attributes such as its dimensions and heading angle. These parameters can not only aid in ship classification [2], but also provide valuable information on the movement direction.

In the open literature there exist several ship size and heading angle estimation methods. One of the most prominent ones is based on the Radon transform [3], [4]. It is an image-based approach where a 2D image containing the object of interest is utilized as input to compute both the size and orientation of the object. Another widely used state-of-the-art method is based on fitting an ellipse to the detected boundary pixels of the ship [5], [6]. However, noisy and sparse border pixels, which may arise due to falsely detected pixels, often lead to an overestimation of the dimension. Morphological operations, e.g., a dilation and an erosion may be necessary for removing these distortions. However, this additional processing effort may not always guarantee reliable results. Furthermore, there exist also deep learning-based approaches which can accurately estimate the ship dimensions, but at the cost of high computation power and the need for a large volume of ship images and ground truth data for training the network [7].

Dr. Sushil Kumar Joshi and Dr. Stefan V. Baumgartner are with the Microwaves and Radar Institute, German Aerospace Center (DLR), and Dr. Björn Tings is with the Remote Sensing Technology Institute, DLR (email: Sushil.Joshi@dlr.de).

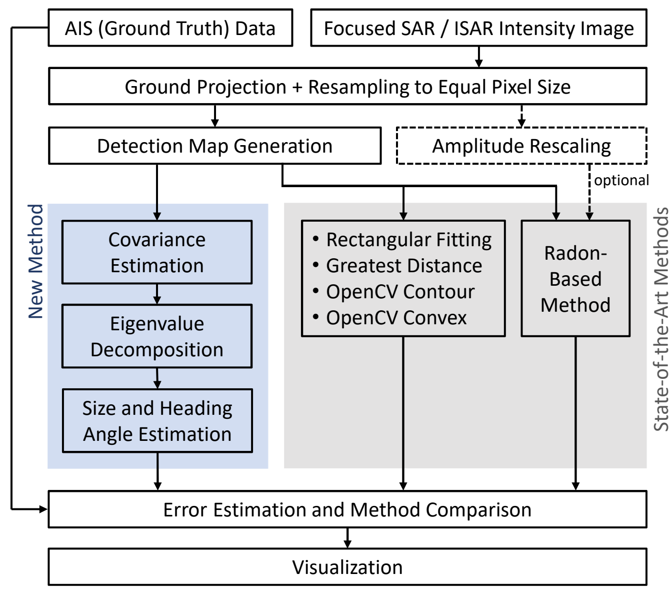

Fig. 1. Framework for performance assessment and comparison of the proposed estimation method (blue color) with state-of-the-art methods (gray).

In this paper a novel computationally fast and accurate ship size and heading angle estimation method is presented. It is suitable for both air- and spaceborne synthetic aperture radar (SAR) and inverse SAR (ISAR) images. Similar to the ellipse-based fitting method discussed previously the proposed method also fits an ellipse to the ship. However, instead of taking just the potentially distorted boundary pixels, it takes into account all the detected pixel positions belonging to the ship for determining its length, beam (= width) and heading angle.

For assessing the performance of the novel method SAR images of ships acquired with TerraSAR-X satellite are used as input and AIS (automatic identification system) [8] data as ground truth. Furthermore, the results are also compared with different state-of-the-art ship size and heading angle estimation methods. The performance assessment framework is shown in Fig. 1. Together with the state-of-the-art methods it is discussed in more detail in the next Section.

II. STATE-OF-THE-ART ESTIMATION METHODS

For accurately estimating sizes and angles of objects in digital image data of any kind it is essential, that the input images have equal pixel size in both dimensions. For SAR images it is also mandatory that they are available in ground range/cross-range geometry. This is ensured by the block *Ground Projection + Resampling to Equal Pixel Size* in Fig. 1.

For the proposed method (cf. block in blue color in Fig. 1) as well as for most of the considered state-of-the-art methods (cf. block in gray color) a binary detection map is needed as input. For ship detection and *Detection Map Generation* generally a constant false alarm rate (CFAR) detection algorithm is applied on the on ground projected[1] input images [9], [10].

For the *Radon-Based* method either a binary detection map or optionally a rescaled intensity/amplitude image can be used as input. This will be explained later in Section IV.

In the following the considered state-of-the-art methods are discussed.

A. Rectangular Fitting

In this method a rectangle with edges parallel to the image x- and y-axes is fitted to the set of ground range and azimuth pixel positions of the ship in the detection map. The maximum and minimum positions in both dimensions are used for estimating the length and beam of the ship, respectively. This approach unfortunately is not capable to estimate the heading angle. For the ship length an underestimation and for the beam an overestimation is generally expected. We have it included anyhow, since it is widely used [5].

B. Greatest Distance

In this method the Euclidean distance between the two farthest pixel positions in the detection map is considered as ship length [11]. The beam of the ship is computed from the greatest distance of the pixels at an angle orthogonal to the line defining the ship length. The Python [12] function *scipy.spatial.distance.cdist* and some functions from the *NumPy* library are used for the implementation of the method.

C. OpenCV-Based Elliptical Fitting

This method fits an ellipse to a set of two-dimensional (2D) points using a least-square approach. The boundary pixel positions of the ship are first extracted either by computing the convex hull or the contour of the ship. In general the convex hull gives less boundary points than the contour. Thus, the contour can lead to more accurate size estimates, especially when the object has concavities or irregularities. For computing the convex hull and the contour the Python functions *sciPy.spatial.ConvexHull* and *skimage.measure.find_contours*, respectively, are used. For fitting an ellipse to the points obtained with these two functions, the function *cv2.fitEillipse* from the *OpenCV* library [13] is used. As output the center, major and minor axes of the fitted ellipse and its orientation is obtained. The major and minor ellipse axes directly correspond to the ship's length and beam, respectively.

[1] Please note that also already available detection maps in slant range geometry can be projected to ground and resampled to equal pixel size. Thus, the CFAR detector not necessarily needs to be applied on SAR images in ground range geometry but also can be applied on SAR images in slant range geometry if subsequently the projection of the detection map to ground and resampling is carried out.

D. Radon-Based Method

This method utilizes the Radon transform [14]. For estimating the heading angle of the ship, which is assumed to be an elongated object, the position of the intensity maximum in the sinogram is considered. The beam and length of the ship are obtained from the thresholded sinogram intensity projections corresponding to the heading angle and the angle orthogonal to the heading angle, respectively [4]. For the practical implementation the Python function *skimage.transform.radon* is used.

III. Proposed Eigen-Based Method

This method is motivated by the concept of confidence ellipses used for describing uncertainties in multivariate normal distributions [15]. Recently in [16] the concept has been used for tracking multiple extended targets using ground-based marine radar. To the best of the authors' knowledge the potential of this method has never been demonstrated for size and heading angle estimation of ships in air- and spaceborne SAR data.

As a first step the covariance matrix is computed using the ship pixel positions obtained from the detection map. Then the eigenvalues and eigenvectors are estimated after performing the eigenvalue decomposition (EVD) of the covariance matrix.

The EVD of the covariance matrix $\hat{\boldsymbol{C}}_{ship}$ is given as [17]

$$\hat{\boldsymbol{C}}_{\mathrm{ship}} = \boldsymbol{V} \lambda \boldsymbol{V}^{-1}, \tag{1}$$

where $\boldsymbol{V}$ and λ are the eigenvectors and eigenvalues, respectively. The largest and smallest eigenvalues correspond to the semi-major and semi-minor axes of the ellipse, respectively, and the eigenvector corresponding to the largest eigenvalue gives the orientation of the ellipse. The Python function *numpy.cov* is used for computing the covariance matrix and *numpy.linalg.eig* for computing the eigenvalues and eigenvectors of the estimated covariance matrix.

After determining the largest and smallest eigenvalues the length $\hat{l}_{\mathrm{ship}}$, beam $\hat{b}_{\mathrm{ship}}$ and the orientation $\hat{\theta}_{\mathrm{ship}}$ of the fitted ellipse w.r.t. the horizontal image axis can be calculated as

$$\hat{l}_{\mathrm{ship}} = 2\sqrt{k_1 \lambda_1}, \tag{2}$$

$$\hat{b}_{\mathrm{ship}} = 2\sqrt{k_2 \lambda_2}, \tag{3}$$

$$\hat{\theta}_{\mathrm{ship}} = \arctan\left(\frac{V_{1,\mathrm{v}}}{V_{1,\mathrm{h}}}\right), \tag{4}$$

where k_1 and k_2 are scale factors, $V_{1,\mathrm{v}}$ and $V_{1,\mathrm{h}}$ are the vertical and the horizontal components of the eigenvector $\boldsymbol{V}_1$, which corresponds to the largest eigenvalue λ_1.

The scale factors k_1 and k_2 determine the confidence interval for taking into account the 2D distribution of the ship pixel positions. Empirically it was found that for the investigated TerraSAR-X dataset a 75% confidence interval, i.e., $k_1 = k_2 = 2.77$, lead to the most accurate results.

Note that many of the image based orientation angle estimation methods deliver angles only in the range from 0° to 180°. Thus, there is a 180° ambiguity when it comes to true heading

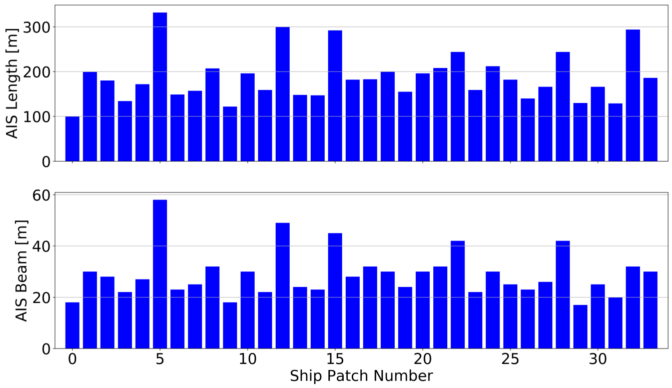

Fig. 2. Actual lengths (top) and beams (bottom) of the 34 investigated ships obtained from AIS data.

angle and moving direction estimation. The estimation methods discussed in the paper cannot discriminate between the front and back of ships. For resolving this ambiguity additional information is required, e.g., the tracked ship positions over time [18] or the line-of-sight velocity obtained via along-track interferometry [19] or space-time adaptive processing [20]. For the performance assessment we have manually eliminated such 180° ambiguities.

IV. Experimental Results and Discussion

For assessing the performance of the proposed method and for comparing it with the state-of-the art methods the framework shown in Fig. 1 is used. The estimation errors are computed as

$$\mathrm{Error} = \mathrm{Estimated\,Value} - \mathrm{True\,Value}, \tag{5}$$

so that an over- and underestimation leads to positive and negative error values, respectively. In this equation the $\mathrm{True\,Value}$ is the value obtained from the AIS ground truth data.

For evaluating the performance of the methods in total 34 fully focused ship image patches acquired with the TerraSAR-X satellite are used. All image patches have a size of 176 x 176 pixels, are projected to ground range and are resampled to 3 m pixel spacing in ground range and azimuth direction. Each image patch contains a ship of a certain size and heading angle for which also AIS ground truth data is available. The actual length and beam values for these ships obtained from the AIS data are shown in Fig. 2. The ship lengths vary between 100 m and 332 m and the beams between 17 m and 58 m, respectively.

All methods, except the *Radon-Based* method, are applied only to the pixel-based detection map of the ship as shown in Fig. 1. For the *Radon-Based* method instead of the detection map also an intensity image can be used as input. However, the intensity of such an image has to be properly normalized or rescaled before applying the Radon transform. The reason for this is the high dynamic range of SAR data, which can be larger than 100 dB. Very bright single scatterers may hide the actual shape of the ship and lead to unreliable size and heading angle estimation results as shown in Fig. 3.

TABLE I
Root mean square error (RMSE) for the Radon-based method for the cases (a), (b) and (c) discussed in Fig. 3. For the RMSE computation all 34 ship image patches were used.

RMSE	Case (a) 0 to -100 dB	Case (b) -40 to -100 dB	Case (c) Detection Map
Length [m]	123.66	38.22	**15.64**
Beam [m]	12.69	12.28	**7.42**
Heading [°]	29.41	3.87	**3.42**

It can be seen in Fig. 3 that an input image normalized and scaled in different ways may yield to completely different estimation results. The root mean square error (RMSE) for these cases using all 34 ship image patches are summarized in Table I. From the bold values in the table it is clearly recognizable that the best results for the *Radon-Based* method are obtained when the binary detection maps are used as input rather than the intensity images itself. Thus, for the later comparison of all estimation methods only the detection map is considered as single input source.

In Fig. 4 the estimation results for three different ship image patches are shown exemplary. It can immediately be seen that the *Rectangular Fitting* method simply creates a bounding box based on the minimum and maximum ship pixel positions and lacks heading angle information. Furthermore, compared to the method based on *OpenCV Contour*, the *OpenCV Convex* method tends to overestimate especially the beam. This is because the former method uses more boundary pixels compared to the latter. Altogether, the *OpenCV Contour*, the *Radon-Based* and the proposed *Eigen-Based* methods seem to fit very well with the ship shapes and orientations for the detection maps shown in Fig. 4.

In Fig. 5 the estimation error results for all 34 available ship images patches are shown. It is evident that the length and beam estimates for all methods tend to either underestimate or overestimate, as expected. This disparity can be attributed to several underlying factors, including the side-looking SAR acquisition geometry, multi-path reflections from the ships to the ocean surface and vice versa, fluctuation of the radar cross section (RCS) and, thus, not accurate representation of the ship shape, and defocusing or smearing effects in the SAR image caused by ship motion. The shown heading angle estimates are very close to the ground truth data with an estimation error better than $\pm 10°$ (cf. Fig. 5 bottom).

Finally the RMSE and, hence, the estimation accuracy for all investigated methods was also computed. The results are listed in Table II. In comparison to the state-of-the-art methods, the proposed *Eigen-Based* method gives the best results with the lowest RMSE values of 12.22 m, 8.64 m and 2.79° for ship length, beam and heading angle, respectively. The second best results are obtained with the *Radon-Based* method and the third best with the *OpenCV Contour* method. Note that for the computation of the Radon transform a step size of 1° and a range from 0° to 180° was used.

Furthermore, a processing time evaluation was also carried out. For each ship image patch of size 176 x 176 in pixels each estimation method was executed hundred times and the average processing times were calculated. The computations

This article has been accepted for publication in IEEE Geoscience and Remote Sensing Letters. This is the author's version which has not been fully edited and content may change prior to final publication. Citation information: DOI 10.1109/LGRS.2024.3402362

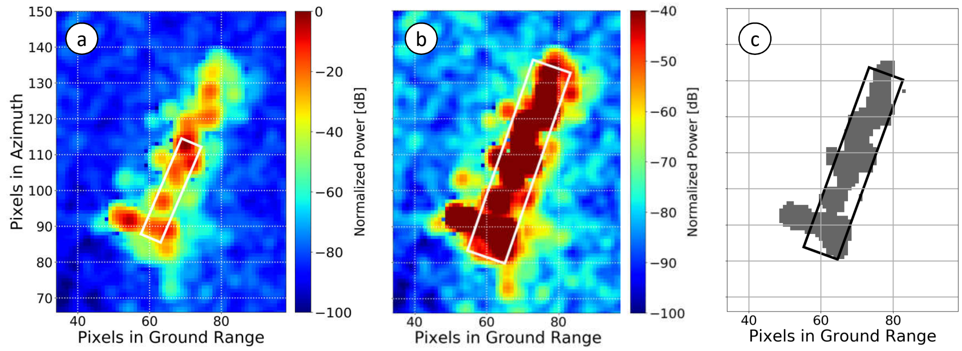

Fig. 3. Radon-based fitting results for image patch no. 10 scaled in different ways before applying the estimation method. The white and black rectangles visualize the estimation results. (a): Image normalized to its maximum value and afterwards rescaled to maximum value of 0 dB and to a minimum of -100 dB; (b): Normalized to maximum and then rescaled to the range of -40 dB to -100 dB; (c): Binary detection map used as input image.

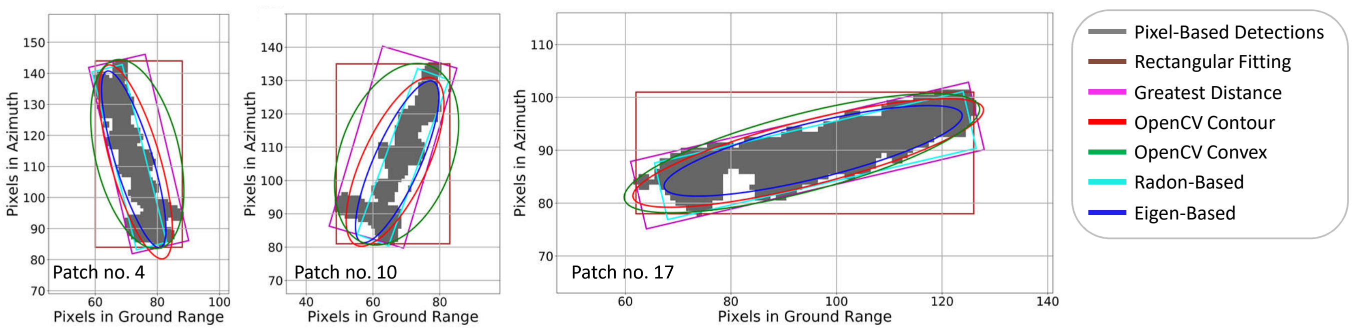

Fig. 4. Some examplary ship size and angle estimation results obtained from the discussed methods superimposed on their respective binary detection maps, which are used as input for the estimation methods. The patch numbers in the figure are shown in Fig. 2. All image patches originally have a dimension of 176 x 176 in pixels but have been truncated for the visualization purposes.

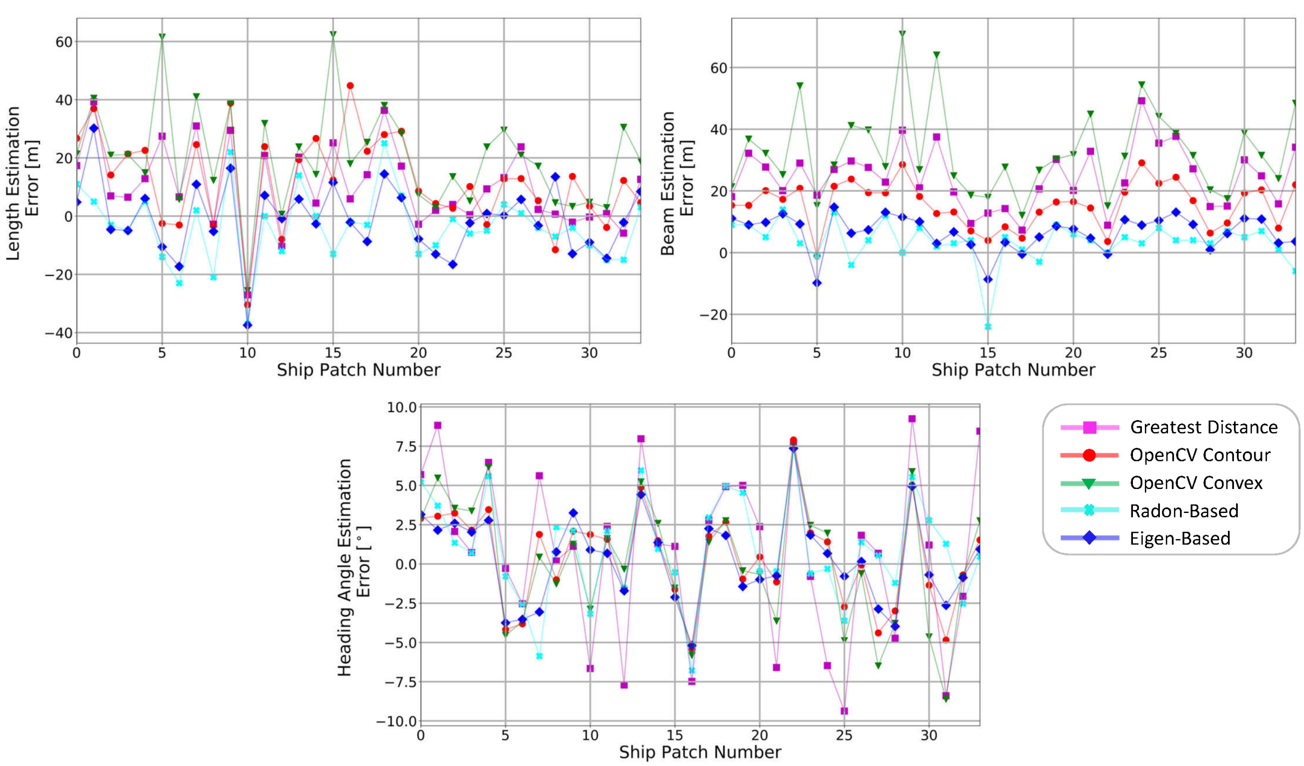

Fig. 5. Length (top left), beam (top right) and heading angle (bottom) estimation errors for all 34 ship image patches. The results from the *Rectangular Fitting* method are not included owing to its large estimation errors and its inability for heading angle estimation.

TABLE II
RMSE AND AVERAGE PROCESSING TIME OF THE ESTIMATION METHODS. THE NUMBERS IN BOLD SHOW THE BEST ACHIEVED ACCURACIES.

Estimation Methods	RMSE (= Achieved Accuracies)			
	Length [m]	Beam [m]	Heading [°]	Processing Time [μs]
Rectangular Fitting	22.62	77.74	n/a	207
Greatest Distance	17.12	26.31	5.37	11000
OpenCV Contour	19.85	17.18	3.07	1061
OpenCV Convex	26.38	35.53	3.94	1012
Radon-Based	15.64	**7.42**	3.42	400000
Eigen-Based	**12.22**	8.64	**2.79**	**112**

were carried out on a conventional personal computer with an Intel(R) Xeon(R) processor E3-1270 v5 running at 3.60 GHz. The processing time results are listed in the most right column of Table II. The proposed *Eigen-Based* method is the fastest among all methods with an average processing time of only $\approx$ 112 μs. More important than the absolute processing time is the fact that proposed *Eigen-Based* method is almost twice as fast as the inaccurate *Rectangular Fitting* method, which is on second position in terms of processing time. The *Radon-Based* method is approx. 3600 times and the *OpenCV Contour* method approx. 10 times slower than the proposed *Eigen-Based* method.

In short both in terms of processing time and estimation accuracy the proposed *Eigen-Based* method surpasses the other investigated state-of-the-art methods, making it an attractive choice for real-time ship monitoring and classification applications.

V. Conclusion

In this paper a novel eigenvalue decomposition-based ship size and heading angle estimation method was proposed. For performance assessment TerraSAR-X SAR image patches of ships and AIS ground truth data were used. Comparative analyses against several state-of-the-art estimation methods revealed that the parameters estimated with the novel proposed *Eigen-Based* method have the highest accuracy. Furthermore, in terms of computation time the proposed method is also the fastest, outperforming, for instance, the state-of-the-art *Radon-Based* method by a factor of 3600 and the *OpenCV Contour* method by a factor of 10. Due to low computational load the method is suitable for real-time ship size and heading angle estimation. We want to point out that the proposed method can also be applied one to one on focused ISAR intensity images of ships, although no ISAR results are shown in the paper.

We intend to integrate the proposed method into our own maritime moving target indication processing framework [21], which will be installed on the onboard computer of the compact multi-channel S-band HAPSAR sensor [22]. This sensor will be integrated as payload in the DLR High-Altitude Platform (HAP) [23].

References

[1] S. Brusch, S. Lehner, T. Fritz, M. Soccorsi, A. Soloviev, and B. van Schie, "Ship Surveillance With TerraSAR-X," *IEEE Transactions on Geoscience and Remote Sensing*, vol. 49, no. 3, pp. 1092–1103, 2011.

[2] C. Bentes, D. Velotto, and B. Tings, "Ship Classification in TerraSAR-X Images With Convolutional Neural Networks," *IEEE Journal of Oceanic Engineering*, vol. 43, no. 1, pp. 258–266, 2018.

[3] Q. Zhang and I. Couloigner, "Accurate Centerline Detection and Line Width Estimation of Thick Lines Using the Radon Transform," *IEEE Transactions on Image Processing*, vol. 16, no. 2, pp. 310–316, 2007.

[4] K.-A. Park, J.-J. Park, J.-C. Jang, J.-H. Lee, S. Oh, and M. Lee, "Multi-Spectral Ship Detection Using Optical, Hyperspectral, and Microwave SAR Remote Sensing Data in Coastal Regions," *Sustainability*, vol. 10, no. 11, p. 4064, 2018.

[5] M. Stasolla and H. Greidanus, "The exploitation of Sentinel-1 images for vessel size estimation," *Remote Sensing Letters*, vol. 7, no. 12, pp. 1219–1228, 2016.

[6] J.-J. Park, K.-A. Park, P.-Y. Foucher, M. Lee, and S. Oh, "Estimation of ship size from satellite optical image using elliptic characteristics of ship periphery," *International Journal of Remote Sensing*, vol. 41, no. 15, pp. 5905–5927, 2020.

[7] Y. Ren, X. Li, and H. Xu, "Extracting Ship's Size from SAR Images by Deep Learning," in *Artificial Intelligence Oceanography*. Springer Nature Singapore Singapore, 2023, pp. 303–321.

[8] B. J. Tetreault, "Use of the Automatic Identification System (AIS) for maritime domain awareness (MDA)," in *Proceedings of Oceans 2005 Mts/Ieee*. IEEE, 2005, pp. 1590–1594.

[9] S. K. Joshi, S. V. Baumgartner, A. B. da Silva, and G. Krieger, "Range-Doppler Based CFAR Ship Detection with Automatic Training Data Selection," *Remote Sensing*, vol. 11, no. 11, p. 1270, 2019.

[10] S. Bocquet, L. Rosenberg, and C. H. Gierull, "Parameter Estimation for a Compound Radar Clutter Model With Trimodal Discrete Texture," *IEEE Transactions on Geoscience and Remote Sensing*, vol. 58, no. 10, pp. 7062–7073, 2020.

[11] B. Tings, C. A. Bentes da Silva, and S. Lehner, "Dynamically adapted ship parameter estimation using TerraSAR-X images," *International Journal of Remote Sensing*, vol. 37, no. 9, pp. 1990–2015, 2016.

[12] G. Van Rossum and F. L. Drake, *Python 3 Reference Manual*. Scotts Valley, CA: CreateSpace, 2009.

[13] J. Howse, *OpenCV Computer Vision with Python*. Packt Publishing Birmingham, 2013, vol. 27.

[14] J. Radon, "Über die Bestimmung von Funktionen durch ihre Integralwerte längs gewisser Mannigfaltigkeiten," *Berichte Sächsische Akademie der Wissenschaften, Leipzig, Mathematisch-Physikalische Klasse*, vol. 69, pp. 262–277, 1917.

[15] T. W. Anderson, T. W. Anderson, T. W. Anderson, T. W. Anderson, and E.-U. Mathématicien, *An Introduction to Multivariate Statistical Analysis*. Wiley New York, 1958, vol. 2.

[16] J. S. Fowdur, M. Baum, and F. Heymann, "An Elliptical Principal Axes-based Model for Extended Target Tracking with Marine Radar Data," in *2021 IEEE 24th International Conference on Information Fusion (FUSION)*, 2021, pp. 1–8.

[17] G. Strang, *Linear Algebra and Its Applications*. Brooks/Cole, 2005.

[18] S. K. Joshi, S. V. Baumgartner, and G. Krieger, "Tracking and Track Management of Extended Targets in Range-Doppler Using Range-Compressed Airborne Radar Data," *IEEE Transactions on Geoscience and Remote Sensing*, vol. 60, pp. 1–20, 2022.

[19] J. H. Ender, C. H. Gierull, and D. Cerutti-Maori, "Improved Space-Based Moving Target Indication via Alternate Transmission and Receiver Switching," *IEEE Transactions on Geoscience and Remote Sensing*, vol. 46, no. 12, pp. 3960–3974, 2008.

[20] W. L. Melvin, "A STAP overview," *IEEE Aerospace and Electronic Systems Magazine*, vol. 19, no. 1, pp. 19–35, 2004.

[21] S. V. Baumgartner and S. K. Joshi, "Onboard Processing Concept for Maritime Surveillance Demonstrated with DLR's Airborne Radar Sensors F-SAR and DBFSAR," in *EUSAR 2021; 13th European Conference on Synthetic Aperture Radar*. VDE, 2021, pp. 1–6.

[22] M. Jirousek, M. Peichl, S. Anger, S. Dill, and M. Limbach, "The DLR High Altitude Platform Synthetic Aperture Radar Instrument HAPSAR," in *EUSAR 2024; 15th European Conference on Synthetic Aperture Radar*, 2024.

[23] F. Nikodem, "Overview of the DLR High Altitude Platform and Scientific Potential of the Technology Demontrator HAP-alpha," in *Deutscher Luft- und Raumfahrtkongress 2023*. DGLR, 2023, pp. 1–7.